

Speckle Fluctuations and Their Use as Probes of Dense Random Media

A. G. YODH,¹ D. J. PINE,² P. D. KAPLAN,¹ M. H. KAO¹ AND N. GEORGIADES¹

¹*Department of Physics, University of Pennsylvania, Philadelphia, PA 19104, USA;*

²*Exxon Research and Engineering Co, Rt. 22 East, Annandale, NJ 08801, USA*

Received and accepted 29 September 1991

A brief review of the underlying principles of diffusing-wave spectroscopy is given, and direct measurements of the path-dependent correlation function are described. In addition we introduce experiments to probe particle motion on very short length ($< 2\text{\AA}$) and time ($< 10\text{ ns}$) scales, and discuss recent measurements of structure and diffusion in dense binary hard sphere fluids.

Keywords: speckle fluctuation, probe, dense random media

INTRODUCTION

In this communication we discuss some exciting new developments connected with multiply scattered speckle fields and their use as probes of dense colloidal suspensions. Since our subject matter is quite different from the mainstream of topics covered in the Nonlinear Optical Symposium,¹ we will review the general principles of the new measurements, and then describe some related work from our laboratory. The goal of this paper is to provide a subjective snapshot of this growing field. Thus, our presentation is swift and informal. The interested reader can pursue details by following up on the references provided.

The properties of multiply scattered light have been of interest to a broad range of scientists for well over a century.² In physics we quite often find ourselves concerned with single-scattering problems for which the theoretical connection between measurement and material characteristics is relatively clear; multiple scattering is a nuisance. On the other hand a very large number of systems in nature scatter light many times. For example, multiple scattering is intimately tied to the white appearance of table salt, clouds, fog, and foam. The phenomenon affects our ability to image through biological tissue and transmit information through the atmosphere. Importantly (with respect to the present paper) this phenomenon also affects our ability to study dense solid, liquid, and gaseous dispersions. This is because the relevant length scales in these dispersions, such as particle size and interparticle spacing, are often comparable to the wavelength of light.

In this paper we focus on a new spectroscopy that has been developed and applied to study the properties of optically dense colloidal suspensions. The technique, called diffusing-wave spectroscopy (DWS) is basically a class of dynamic, or quasi-elastic, light scattering (QELS) experiment that is applicable to systems that multiply scatter light.³⁻⁵ DWS is exciting for several reasons.

First, it offers the possibility to experiment with new systems. Progress in our understanding of dense colloids has lagged that of dilute colloids (at least in part) as a result of multiple scattering. With this new probe we can look forward to probing the dynamics of strongly interacting colloidal structures (e.g. volume fractions, $\phi > 0.1$), and ultimately improving our understanding of the roles played

by Coulombic, steric, hydrodynamic, and hard-sphere interactions in producing these structures.

Second, it turns out that one can use the probe to re-examine the Brownian dynamics of a single isolated particle suspended in a fluid⁶ on new length and time scales. The key quantity of interest here is the average particle displacement, and its variation as a function of time. The shortest length scales probed by single scattering measurements⁷⁻⁹ are set by the wavelength of the incident light beam ($\sim 5000 \text{ \AA}$). However, after a particle has moved 5000 \AA its diffusive motion is well established. The shortest length scales probed by the multiple scattering measurements are set by the probe wavelength divided by the square root of the number of random walk steps taken by a typical photon diffusing through the medium. The number of random walk steps can be made very large enabling the experimenter to study particle motions on length scales of $\sim 10 \text{ \AA}$ and lower. In this time regime the particle motion is evolving from purely ballistic to diffusive behaviour. A full theory of this phenomena must directly couple particle motion to the hydrodynamic degrees of freedom of the surrounding fluid.¹⁰

Finally, the fluctuation and transport properties of multiply scattered light are interesting in their own right. There are a number of important problems in this area. We are particularly interested in understanding the breakdown of DWS as, for example, the number of scattering events decreases. In addition, we are trying to elucidate further the role of material structure in affecting the properties of the diffuse light fields. Problems of photon localization,¹¹ and speckle statistics¹² are also related to the phenomena we discuss here, and have been the subject of intense effort recently.

DIFFUSING-WAVE SPECTROSCOPY: BASIC IDEAS

In this section we derive the basic results needed to understand a DWS measurement. A typical sample in these experiments consists of a suspension of polystyrene spheres in water. The particles have diameters between ~ 0.05 and $\sim 3 \mu\text{m}$, and for the purposes of this exposition we will assume they are hard spheres. The concentration, size, and refractive index of the spheres controls the scattering rate in our samples.

Suppose we wish to investigate the Brownian dynamics of the particles in a dilute system. If the sample is dilute enough, a photon scatters on average less than once when traversing the medium, and we can perform a standard quasi-elastic light scattering (QELS) measurement.⁷⁻⁹ In this measurement the sample is illuminated with a monochromatic input light field possessing a well-defined propagation vector, \mathbf{k}_{in} . In the presence of this field each particle acts like a oscillating dipole, and thus radiates some output field. A detector located in the far field points toward the sample along a particular direction, and thus defines an output propagation vector, \mathbf{k}_{out} . In the case of quasi-elastic scattering, $|\mathbf{k}_{\text{in}}| = |\mathbf{k}_{\text{out}}| = k_0$, and the total field at the detector surface is a superposition of all radiated particle dipole fields. Since the particles move, the relative phase between individual fields changes in time, and the measured intensity fluctuates.

Information about the sample is most easily obtained by measuring the temporal autocorrelation function of the scattered electric field. For independent particles undergoing Brownian motion it is easy to show⁷⁻⁹ that this autocorrelation function decays exponentially in time at a rate proportional to $q^2 \langle \Delta r^2(\tau) \rangle$. Here $\langle \Delta r^2(\tau) \rangle$ is the mean square particle displacement during the time interval τ , and $q = |\mathbf{k}_{\text{out}} - \mathbf{k}_{\text{in}}| = 2k_0 \sin(\theta/2)$ is the scattering wavevector for the particular experimental geometry used (θ is the scattering angle.) One can learn considerably more about the suspension with this type of measurement,⁷ but the main points we stress here are that sample information is derived from the *autocorrelation* function of the scattered field, and that the fluctuation time that characterizes the decay of this field

correlation function is equal to the time it takes a particle to move a distance $\sim 1/q$. Note that $1/q$ is of the order of the probe wavelength λ or larger.

Diffusing-wave spectroscopy is also a quasi-elastic light scattering measurement, but under drastically different circumstances: (1) the particle concentration is made very large, and therefore (2) the light is multiply scattered. Incident photons diffuse through the dense colloid, hence the name 'diffusing-wave spectroscopy'. The experimental apparatus is fairly simple (see Figure 1). A light field illuminates the front face of a cuvette of thickness L , containing a dense colloid. A complicated interference or speckle pattern is produced at the output plane of the cell. If the particle positions were fixed, then the speckle pattern would be static, but since the particles move, the pattern at the output face fluctuates in time. In our experiments we collect a single, diffraction limited output speckle, and measure its temporal correlation function. This is quite similar to the single scattering experiment. The major advance of DWS lies in the development of quantitative relations between the correlation functions of the multiply scattered speckle field and the density fluctuations within the sample.

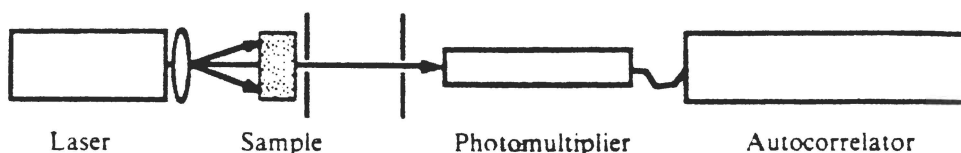


FIGURE 1 Schematic of a typical DWS measurement. Light from a laser is directed onto a cuvette containing a dense colloidal suspension. Each photon travels through the sample along a complicated path. At the output face a portion of the emerging speckle field is directed onto a photomultiplier tube, and the intensity autocorrelation function of the speckle is computed using standard photon correlation electronics.

In order to best understand these ideas it is useful to begin by considering the properties of an electric field produced by photons travelling along a single trajectory through the sample. The trajectory must begin at the point where we deposit our incident photons, and must end at our output collection point where the photons emerge. Microscopically one can envisage each photon travelling ballistically between particles, and experiencing changes in propagation direction after each scattering event. Three important length scales characterize the photon transport in this picture: (1) s , the total distance travelled by the photon; (2) l , the mean distance between particle encounters; and (3) l^* , the transport mean free path of the photon. The distance l is determined primarily by the total scattering cross-section and number density of the constituent particles. The transport mean free path, l^* , corresponds to the distance a photon travels in the media before its wavevector is completely randomized. Thus l^* is the random walk step-size for the diffusing photons; it depends primarily on l and the *differential* scattering cross-section of the particle. For micrometer size spheres, l^* is usually several times larger than l and ranges from ~ 10 to $> 100 \mu\text{m}$ in our experiments. The most probable total path-length, s , scales as (L^2/l^*) , and can be of the order of several centimeters for 1 mm-thick sample cells.

This ray picture¹³ works remarkably well in providing expressions for the field correlation functions. We now outline the basic steps in their derivations. First we assume that the photon experiences a momentum change $q_j = k_{j+1} - k_j$ as a result of scattering from the j th particle at position r_j in the sample. If there are $N = s/l$ scattering events then we can write the phase of the electric field, $E_i(t, s)$, along this trajectory as a *product* of phase factors for each scattering event, i.e.

$$E_i(t, s) \sim e^{-i\omega t} \prod_{j=1}^N e^{iq_j \cdot r_j(t)} \quad (1)$$

The total speckle fields, $E_T(t)$, due to all paths of length s through the sample will be a sum of *path-dependent* fields of the form in Equation 1, i.e. $E_T(t) = \sum_i E_i(t,s)$. Information about the particle dynamics are derived from the *path-dependent* temporal autocorrelation function, $g_1^s(\tau) = \langle E_T^*(t+\tau)E_T(t) \rangle / \langle |E_T(t)|^2 \rangle$, of the total speckle field, where $\langle \dots \rangle$ represent a time average. The problem is now formulated in a general way, and a number of simple assumptions enable us to calculate $g_1^s(\tau)$.

First we assume that the individual $E_i(t,s)$ are uncorrelated. This is not strictly correct, but the higher order corrections have been estimated by field theoretic methods¹⁴ and are quite small for the experimental geometries used in typical DWS measurements. If, in addition, we assume that the particles are non-interacting, then we conclude that

$$g_1^s(\tau) = \langle e^{-i\omega\tau} \prod_{j=1}^N e^{i\mathbf{q}_j \cdot \Delta\mathbf{r}_j(\tau)} \rangle_{\text{one path}} \quad (2)$$

Here $\Delta\mathbf{r}_j(\tau)$ is the displacement of the j th particle during the time τ . The product of phase shifts can be simplified dramatically if successive phase shifts along the trajectory are uncorrelated. Then we can replace the product of phase shifts with the *average single particle phase shift* raised to the power N .

$$g_1^s(\tau) = e^{-i\omega\tau} \left[\langle e^{i\mathbf{q} \cdot \Delta\mathbf{r}(\tau)} \rangle_{\text{single event}} \right]^N \quad (3)$$

The complicated problem has thus been reduced to a calculation of the average value of, $e^{i\mathbf{q} \cdot \Delta\mathbf{r}(\tau)}$, for a 'typical particle' in the scattering pathway. However, \mathbf{q} and $\Delta\mathbf{r}(\tau)$ are different for each scattering event, and we must average over all allowed momentum transfers and particle displacements. Certainly \mathbf{q} is no longer a quantity that is well defined by experimental geometry. To solve this problem we make the assumption that \mathbf{q} and $\Delta\mathbf{r}(\tau)$ are independent variables. Again this assumption cannot strictly be true since we use a fixed input/output geometry for the photons, so that if the particles move, we effectively demand that the scattering \mathbf{q} s change too. However, one can again show by calculation¹⁵ that for the present experiments the first order dynamical correction as a result of this breakdown is very small (essentially undetectable.) We further assume that the particle displacement is a centred, random Gaussian variable, and perform the $\Delta\mathbf{r}(\tau)$ average to obtain,

$$g_1^s(\tau) = e^{-i\omega\tau} \left[\langle \exp\{-(1/6)q^2\langle\Delta r^2(\tau)\rangle\} \rangle_{q, \text{single event}} \right]^N \quad (4)$$

In any practical DWS experiment the argument of the decaying exponential in Equation 4 will be $\sim 1/N$. Thus, it is reasonable to perform the q -average on only the first-order term in the expansion of the exponential, and we arrive at the fundamental result for the path-dependent correlation function:

$$g_1^s(\tau) = e^{-i\omega\tau} \left[\exp\{-(1/6)\langle q^2 \rangle \langle \Delta r^2(\tau) \rangle\} \right]^N \quad (5)$$

Here $\langle q^2 \rangle$ is the mean square scattering vector for a single scattering event in the sample. For independent particles it is straightforward to show that $\langle q^2 \rangle = 2(k_0)^2 (l/l^*)$ so that,¹³

$$g_1^s(\tau) = e^{-i\omega\tau} \exp\left[-k_0^2 \langle \Delta r^2(\tau) \rangle (s/l^*)/3\right], \text{ where } N = s/l. \quad (6)$$

Notice that $g_1^s(\tau)$ decays by $1/e$ when the average particle displacement is $\sim \lambda/(s/l^*)^{1/2}$.

All dynamic light scattering correlation functions decay in the time it takes the phase of the scattered field to change by $\sim \pi$. In single scattering experiments this occurs when a typical particle position changes by $l/q (> \lambda)$ along the direction defined

by q . In the multiple light scattering experiments this occurs when the total particle displacement projected along the direction of the output speckle wavevector changes by $\sim \lambda$. Since the scattered photons encounter many particles before emerging from the sample, the distance that each particle must move is much less than λ . Loosely speaking we can associate a phase shift of $k_0 \Delta r(\tau)$ with each step in the photon random walk. Since the direction of $\Delta r(\tau)$ is random, the total phase shift along any particular direction will scale as the square root of the number of photon random walk steps. Equation 6 is a quantitative statement reflecting this simple idea.

In practice the measured DWS correlation functions depart significantly from the result in Equation 5. This is because in a real experiment there are *many photon pathlengths* that contribute to the output speckle field. The distribution of pathlengths depends on details such as experimental geometry, absorption, etc. CW measurements are sensitive to the *total* electric field autocorrelation function, $G_1(\tau)$, which is computed by incoherently summing the contributions of each path-dependent $g_1^s(\tau)$ weighted by $P(s)$, the probability that a photon will travel a distance s through the medium, i.e.

$$G_1(\tau) = \int_0^\infty g_1^s(\tau) P(s) ds = \int_0^\infty P(s) e^{-i\omega\tau} \exp[-k_0^2 \langle \Delta r^2(\tau) \rangle (s/l^*)/3] ds. \quad (7)$$

For purely Brownian motion, $\langle \Delta r^2(\tau) \rangle = 6D\tau$ where D is the particle self-diffusion constant, and we see from Equation 7 that $G_1(\tau)$ is the Laplace transform of $P(s)$ with appropriate scale factors. Using the diffusion equation one can calculate $P(s)$ for various experimental geometries^{13,16} such as plane-wave-in/point-source-out, or point-source-in/point-source-out, etc. In fact it is essential to incorporate the correct $P(s)$ function or the estimated diffusion coefficients will be incorrect. We note also that, in practice, the photon correlation experiments measure an *intensity* autocorrelation function, $G_2(\tau)$, rather than the field correlation function, and that the two are assumed to be related through the Siegert relation,⁹ $G_2(\tau) = 1 + \beta |G_1(\tau)|^2$.

RECENT PROGRESS

In this section we describe some results we have obtained in our laboratory. Once again our desire is to provide a flavour for the types of problems one can hope to address. Therefore many of the results are preliminary. We first discuss our direct measurements of the path-dependent correlation function, then we comment on some new experiments we are performing to measure particle displacements smaller than 2\AA , and finally we describe some work on interacting colloids.

Direct Measurement of the Path-dependent Correlation Function

In the previous section we derived a rather simple expression for the path-dependent speckle field correlation function $g_1^s(\tau)$. It is desirable to verify directly that Equation 6 is correct. Until recently all DWS measurements have been made with cw lasers, so that it was essential to incorporate the proper functional form of $P(s)$ in Equation 7 in order to correctly interpret experimental results. We have developed a pulsed variant of the original DWS apparatus that enables us to verify directly the primary theoretical result of the original DWS theory (Equation 6), and ultimately sharpen the resolution of DWS by isolating the contributions of specific photon pathlengths to the autocorrelation function.¹⁷ This method is discussed in detail elsewhere,¹⁷ so we will describe the basic ideas in words, and then point out our key results.

Our experiment takes advantage of nonlinear optical gating in a qualitatively new way. We employ a laser that emits a 100 MHz train of identical, temporally short

(~ 90 ps, $\lambda = \omega/c = 1.06 \mu\text{m}$) light pulses to irradiate our colloidal suspension. Any single pulse that is incident on the sample emerges from the sample with a considerably longer duration. The output *sample* pulse is 'stretched' in time, and its time averaged intensity profile has the same shape as the path-dependent probability function, $P(s)$, in Equation 7. The output sample pulse is then combined in a nonlinear crystal with a *reference* pulse derived from the same laser. As in all optical gating experiments, the reference pulse remains temporally short, and its temporal delay with respect to the sample pulse is carefully controlled. A train of upconverted (second harmonic, SH) pulses is produced in the nonlinear crystal and detected by a photomultiplier tube. If s' is the difference in path-length between the reference and sample arms when the sample is removed, then each pulse within the SH train will have a field $E(2\omega, \tau)$, proportional to the reference field, $E_R(t)$, and the path-dependent scattered field $E_0(t, s')$. When fluctuations in the reference field are negligible, $E_R(t) = E_R$, we have

$$E(2\omega, \tau) \sim E_R E_0(t, s'). \quad (8)$$

In contrast to previous gating experiments¹⁸ we now *measure the temporal autocorrelation function of the upconverted photons*. For most cases of interest, the time scale of the fluctuation in the phase of $E_0(t, s')$ is a much longer source repetition rate, and the duration of the stretched pulse is $\sim 10\times$ shorter than the laser repetition rate. Under these conditions the graininess of the sampling process is unimportant, and the autocorrelation function of the SH photons is given by

$$g_1(2\omega, \tau) \sim \langle E_0^*(t + \tau, s) E_0(t, s) \rangle / \langle |E_0(t, s)|^2 \rangle \sim g_1^s(\tau), \text{ with } s = s'. \quad (9)$$

Notice that the SH electric field will experience the same fluctuations due to particle motion as the scattered electric field for a single pathlength. By varying the pathlength difference, s' , between the sample and reference arms, the reference pulse 'gates' the electric field $E_0(t, s)$ so that only a very narrow range of photon paths centred about $s = s'$ contribute to the fluctuations of the upconverted field (the actual range of paths is determined by the temporal width of the reference pulse.) The autocorrelation function of the SH field is simply the integrand of Equation 7 evaluated at the appropriate s . The temporal behaviour of the autocorrelation function no longer depends on the shape of $P(s)$ and, for fixed s , a plot of $\ln[g_1(2\omega, \tau)]$ versus τ directly yields the time dependence of $\langle \Delta r^2(\tau) \rangle$. In DWS any process that affected $P(s)$, such as the sample geometry or absorption, modified the temporal decay of the measured autocorrelation function. Since the pulsed method is insensitive to $P(s)$ these types of problems are eliminated.

An important additional feature of this scheme is that the dependence of the average SH intensity on the reference delay s , is proportional to $P(s)$. Thus we can directly measure $P(s)$ for any geometry. By fitting the results to predictions of photon diffusion theory, we can experimentally determine l^* and the sample absorption.

The most important physical results of this work are shown in Figure 2. In the inset of Figure 2 we plot the log of the time varying part of a typical SH intensity autocorrelation function $|g_1(2\omega, \tau)|^2$ versus τ . The sample used in this case was a suspension of $0.460 \mu\text{m}$ diameter polystyrene spheres in water. The volume fraction of spheres was 0.3 and the sample thickness was 2 mm. The decay curves were taken at two delays: $s = 7$ cm, and $s = 13$ cm. In contrast to the DWS measurements these curves decay exponentially. This is the expected result when the particle is moving diffusively (see Equation 6.)

Using this sample we performed similar measurements at other values of optical delay. The results of these experiments are summarized in the main part of Figure 2. Here we plot the slope, Γ_1 , of the $\ln|g_1(2\omega, \tau)|$ versus τ curve as a function of s . Within the limitations of the apparatus the measurements corroborate the primary

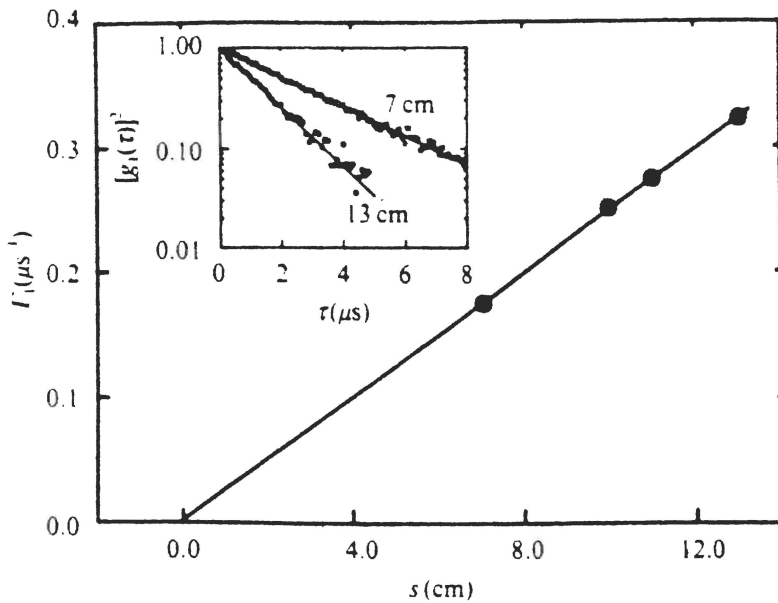


FIGURE 2 Plot of the decay rate of Γ_1 of the upconverted temporal field autocorrelation function versus reference arm delay s . The solid line is a least-squares fit to the data. Inset: plot of the upconverted intensity autocorrelation function versus τ for $s = 7.0$ cm and $s = 13.0$ cm. Both curves exhibit the expected single-exponential decay.

result of DWS. That is, the path-dependent electric field correlation function decays exponentially at a rate proportional to s .

Very-Early Time Particle Diffusion

It was pointed out above that one of the frontiers of DWS is its use as a probe of particle motion on very short length scales. This is possible because the correlation function (see Equation 6) decays by $\sim 1/e$ when particles have moved a distance of $\sim \lambda(s/l')^{1/2}$. In principle we can make this distance smaller and smaller by using thicker and thicker sample cells until the particle no longer moves diffusively. Indeed a recent quantitative DWS experiment¹⁹ has demonstrated that it is essential to incorporate a full hydrodynamic picture of particle interactions when considering particle motion in the non-diffusive regime (e.g. when $\langle \Delta r^2(\tau) \rangle$ does not depend linearly on time.) Further work along these lines can be anticipated because these types of problems have not been studied quantitatively, and it appears highly desirable to push these measurements into shorter and shorter time regimes.

All DWS measurements performed thus far have been carried out in time domain using standard photon correlation techniques. However, probing shorter and shorter time regimes becomes more difficult with photon correlation techniques since they are ultimately limited by the finite bandwidths of photomultiplier tubes and other detection electronics. On the other hand, no experiments have been reported which measure the fluctuation spectra in the frequency domain. This is probably because of the difficulties that arise in inverting the data and then extracting meaningful information from the wings of the spectral lines. Thus, although one of the most important new physical applications of DWS is connected with trying to understand very early time Brownian motion, to our knowledge all of the experimental efforts to push to shorter times have focused on using faster photon correlators. Presently the smallest bin width in a commercially available photon correlator is 12.5 ns.

We have developed a qualitatively different approach for measuring these correlation functions which can, in principle, enable the experimenter to study variations

in the correlation function on the femtosecond time-scale.²⁰ Our approach combines diffusing-wave spectroscopy with Michelson interferometry. It is yet one more application of the Michelson interferometer, which appears to be quite practical in the context of DWS, and early time particle dynamics. In essence the experimenter measures the *field visibility*^{20,21} of the sample output speckle with a Michelson interferometer. The measurement is in the time-domain where the connection to mean square particle displacement is clear, and, in addition, the measurement provides direct information on the more fundamental *electric field* correlation function, which is usually derived from *intensity* autocorrelation measurements using the Siegert relation.⁹ We call the new method diffusing-wave interferometry (DWI).²⁰

Our current apparatus (a 2 m interferometer) enables us to probe particle motion on short length ($< 2 \text{ \AA}$) and time ($< 10 \text{ ns}$) scales. In Figure 3 we show some preliminary results. Our sample consists of 0.205 \mu m -diameter polystyrene spheres in water. The volume fraction of the spheres is relatively low, $\phi = 0.03$, but the sample is 5 cm thick so that out of 5 W of incident laser power at 5145 \AA , we collect only about 200 photoelectrons per second. In Figure 3 we plot the root-mean-square particle displacement as a function of time. The data are obtained by using the interferometer to measure a correlation function of the form in Equation 7, and then inverting the data to find the best value of $\langle \Delta r^2(\tau) \rangle$. Notice that the particle has moved $\sim 2 \text{ \AA}$ after 10 ns, and that we can resolve substantial changes in the nature of the particle motion. The multiple scattering probe enables us to use $\sim 5000 \text{ \AA}$ light to observe $\sim 2000 \text{ \AA}$ diameter particles move less than 2 \AA !

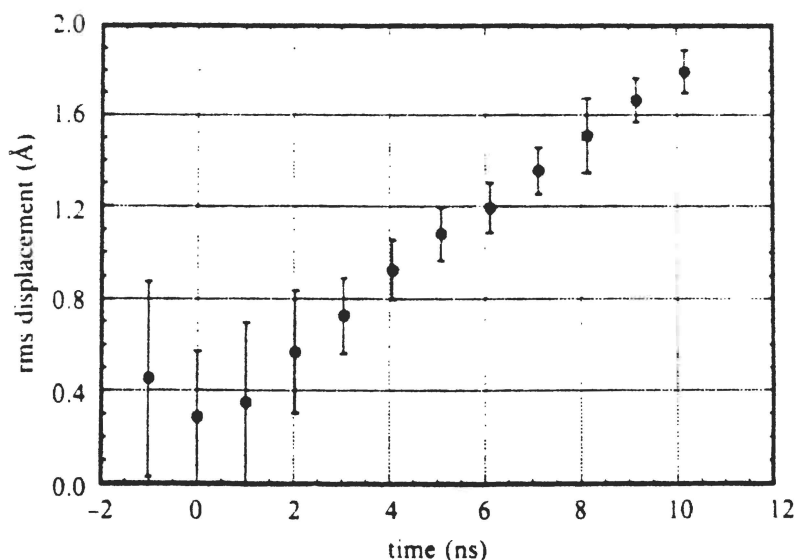


FIGURE 3 Root-mean-square particle displacement as a function of time for 0.205 \mu m -diameter polystyrene spheres in water ($\phi = 0.03$). The data were obtained by inverting the measured electric field autocorrelation function (measured by DWI), and finding the value of the mean square displacement that gave the best fit to the measured correlation function.

Although the data are still preliminary we note that in this regime one can study qualitatively new aspects of the Brownian motion problem. These aspects require a more complete understanding of the mechanisms by which the particle dynamics are coupled to the hydrodynamic degrees of freedom of the fluid.^{10,22} For example, during a time-scale that is less than the fluid viscous damping time, but greater than the time for sound to travel a particle diameter, the particle moves ballistically with a hydrodynamic *effective mass* that is different from the particle *bare mass*. We are involved in measurements to examine these and related issues experimentally for the first time.

Interacting Hard-Sphere Colloids

Our new-found ability to study particle diffusion in dense colloids presents us with the possibility to understand the complex particle interactions that determine the properties of these systems. Our discussion thus far has basically ignored particle interactions, but clearly it is important to begin to include the effects of material structure in our treatment of the multiply scattered light. The first work of this nature has been carried out in connection with monodisperse colloids.^{23,24} We refer the reader to these papers and reference²⁵ for the complete details of this formalism. Presently, we will qualitatively discuss the ideas that are involved, and then give some more complex examples from our laboratory which illustrate the full application of these theories.

We measure two quantities in our experiments: l^* , the photon transport mean free path, and D , some effective particle diffusion constant. Generally, l^* depends only on interparticle structure, while the measured D will depend on interparticle structure and dynamics. Let us discuss l^* first. Thus far we have treated l and l^* as parameters. The connection between l and l^* arises in a variety of random-walk problems such as the problem of directed polymers, and of course the diffusive transport of light. The common feature that emerges from all these treatments is that

$$l^* = l / (1 - \langle \cos \theta \rangle). \quad (10)$$

In light scattering l is the mean distance travelled by the photon before it scatters from a particle. The evaluation of $\langle \cos \theta \rangle$ is harder, but we can easily understand its meaning in the context of dilute (but still multiply scattering) colloids. In this case we envisage the photon travelling relatively long distances ($\sim 100 \mu\text{m}$) before scattering from a single particle. The momentum transfer, $q = |\mathbf{k}_{\text{out}} - \mathbf{k}_{\text{in}}| = 2k_0 \sin(\theta/2)$, that accompanies each scattering event is well defined and we have

$$l^* = l / (1 - \langle \cos \theta \rangle) = l / \langle 2 \sin^2(\theta/2) \rangle = 2(k_0)^2 l / \langle q^2 \rangle. \quad (11)$$

The quantity $\langle q^2 \rangle$ is just the average value of q^2 for a given scattering event. This can be calculated by computing a weighted average q^2 , where the weighting factor is the form factor, $F(q)$, of the particle. The form factor is obtained from Mie scattering theory.²

The next level of complication arises when we introduce short-range correlations into the colloidal suspension. In this case it is useful to imagine the photon travelling relatively long distances through the medium and then scattering from small correlated 'groups' of particles. This picture is reasonable provided that the correlation length or size of each group of particles is small compared to l and l^* . If this is the case we arrive at essentially same result as in Equation 11, except now the q -average must be weighted by the product of the single particle form factor, $F(q)$, and the material structure factor, $S(q)$. Thus we see that the transport properties of light are related to the material structure, but it turns out that the explicit connection involves a q -average, and some information is lost (with respect to single scattering).

The dynamical measurements amount to determining the initial decay rate or first cumulant of our electric field autocorrelation function. In single scattering experiments on non-interacting systems the initial decay rate directly gives the single particle self-diffusion coefficients. On the other hand when the particles interact, even this diffusion constant can depend on q through the material structure factor $S(q)$ as well as through the material hydrodynamic (q -dependent) factor, $H(q)$.^{7,26} The DWS correlation functions provide q -averaged information on these quantities. For large particles the weighted averages can be particularly sensitive to the large- q value (i.e. essentially infinite- q) of these quantities. If the structure is not important (i.e. particle

interactions are weak) the measurements provide information on the free particle diffusion constants.

Recent DWS experiments have focused primarily on the observation of concentration-dependent particle diffusion in monodisperse systems.^{23,24,17} We have been working on related problems in colloids composed of binary hard spheres. The asymmetric binary colloids present us with fundamental geometric questions about particle packing and interparticle forces. In contrast to the uniform dispersions, the interparticle forces in binary colloids depend on the relative sizes and concentrations of the constituent particles. This extra degree of freedom produces a much richer variety of phases and phenomena.²⁷⁻³⁰ As a first step towards addressing these issues we have undertaken a systematic study of the diffusion and structure of binary hard-sphere colloids. Our work aims toward extending DWS to even more complex systems. Below we describe some preliminary results on structure and dynamics in these novel systems.

The experimental apparatus we use is basically the same as in Figure 1. Samples of 1 mm or 0.5 mm thick cuvettes are illuminated from one side by the 514 nm line of a cw Ar-ion laser, and the intensity fluctuations of a single speckle are monitored. We measure l^* by comparing the average transmitted intensity to values obtained from well-understood monodisperse samples, and we extract an effective diffusion constant D_{eff} from the first cumulant of the intensity autocorrelation function decay curve. Measurements are made on mixtures of polystyrene spheres with different particle diameters. In each experiment the volume fraction of large spheres (ϕ_L) is held constant and the volume fraction of small spheres (ϕ_S) is increased from zero to about 0.3.

In Figure 4 we plot the reciprocal of the measured transport mean free path as a function of small sphere volume fraction for two different hard sphere systems. The solid lines are the predicted variation derived using structure factors, $S(q)$, from Percus-Yevick (PY) theory.³¹ The dashed lines are derived from essentially the same theory, except we ignore structural interactions *between unlike spheres*. The ratio of

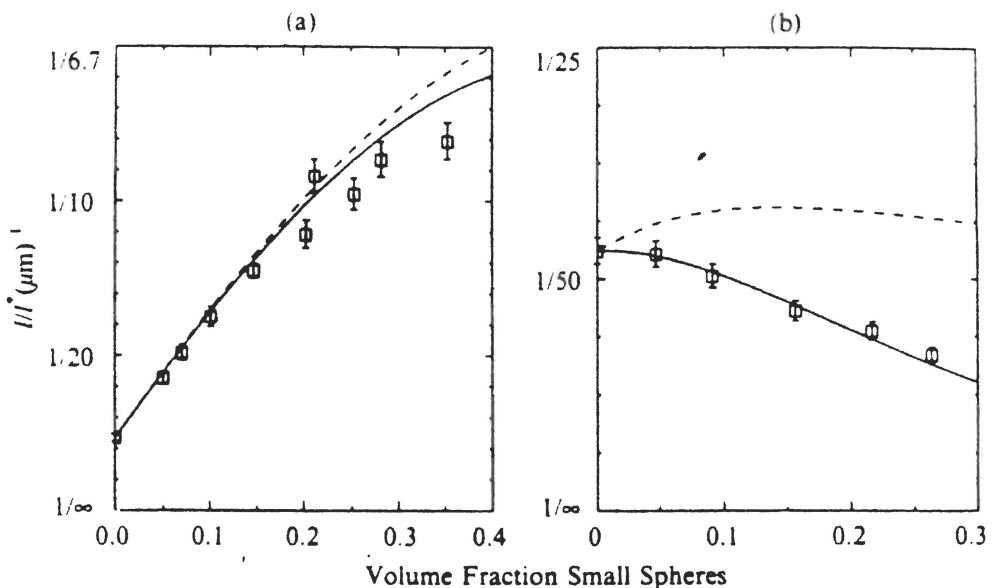


FIGURE 4 The inverse photon mean free path is plotted against volume fraction of small spheres for two systems. In (a) the volume fraction of the $2.0 \mu\text{m}$ -diameter large spheres is fixed at 0.10, and the $0.625 \mu\text{m}$ -diameter small sphere volume fraction is varied. The data almost fall on a straight line as expected in the absence of interparticle interactions. In (b) the large spheres (diameter = $0.205 \mu\text{m}$ -diameter) occupy a volume fraction of 0.045 while the volume fraction of small spheres (diameter = $0.065 \mu\text{m}$) is varied. Here we see the effects of interparticle structure which cause the graph to slope downwards; a non-interacting theory would predict a straight line with a positive slope.

ball diameters in the two experiments is the same (~ 3). In a first approximation $1/l^*$ should vary linearly with the scatterer number density. Deviations from simple lines are a result of particle ordering ($S(q)$), which decrease the optical resistance. We see that the large particle system (Figure 4(a)) basically follows these trends. However, the simple ideas break down significantly in the small particle system (Figure 4(b)). Physically this phenomena is most apparent when the probe wavelength is larger than the small sphere diameter. Notice, however, that the exact theory, which includes correlations between unlike spheres still predicts the data correctly. The striking agreement between theory and experiment gives us confidence that DWS can indeed be used as a sensitive probe of interparticle structure.

Our results on particle diffusion are more difficult to describe without a substantial digression. Nevertheless, these aspects of our experiments are also quite promising. In Figure 5 the effective diffusion constant is plotted as a function of a small sphere volume fraction in the large particle system. It is possible to show that D_{eff} is a weighted average of the diffusion constants for each sphere. In the high- q limit one can derive^{32,33} an exact expression (to first order in particle volume fraction) for D_{eff} . This theory predicts the variation of the solid line in Figure 5. Theories that ignore hydrodynamic coupling between unlike spheres (dashed line), and all spheres (dotted line) are also shown for comparison. With these experiments we are able to test the hydrodynamic coupling coefficients in the theory of unlike spheres for the first time.

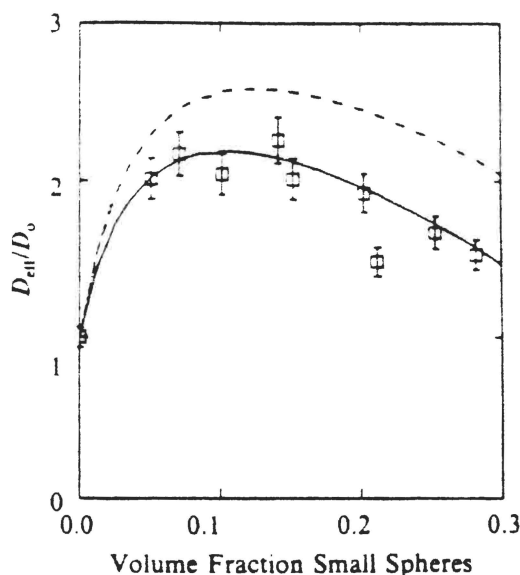


FIGURE 5 The measured diffusion constant, for the 2.00/0.625 μm -diameter system in Figure 4(a), normalized by its value for a system with no small spheres, shows the sensitivity of DWS to interparticle interactions. The solid line is a theory which includes those interactions. The dashed line includes only interactions between particles of the same size. The dotted line ignores all interparticle interactions.

CONCLUSIONS

We have discussed the method of diffusing-wave spectroscopy in some detail, and we have tried to demonstrate its utility as a new probe of dense colloidal suspensions with examples from our laboratory. Many interesting experiments remain. Most work up to now has centred on colloidal suspensions, but recently the methods have been extended to foams.³⁴ It appears the field will continue to be fruitful and exciting for years to come.

ACKNOWLEDGEMENTS

This work was supported by the NSF through grant #DMR-9003687, through the MRL program #DMR-8519059, and through a Presidential Young Investigator Award (AGY). One of us (AGY) acknowledges partial support from the Alfred P. Sloan Foundation, AT&T, and Hercules Inc.

REFERENCES

1. This paper was presented at *The Symposium for Nonlinear Optics of Organic and Polymer Systems and Photonic Devices*, Program Chair. A. F. Garito, April 29–30, Philadelphia, PA 1991.
2. See for example, A. Ishimaru, *Wave Propagation and Scattering in Random Media Vol 1* (Academic Press, New York, 1978).
3. M. J. Stephen, *Phys. Rev. B*, **37**, 1 (1988).
4. G. Maret and P. E. Wolf, *Z. Phys. B*, **65**, 409 (1987).
5. D. J. Pine, D. A. Weitz, P. M. Chaikin, and E. Herbolzheimer, *Phys. Rev. Lett.*, **60**, 1134 (1988).
6. See for example S. Chandrasekhar, *Rev. Mod. Phys.*, **15**, 1 (1943) and references therein.
7. P. N. Pusey and R. J. A. Tough, in *Dynamic Light Scattering*, R. Pecora ed., 85 (Plenum, New York, 1985).
8. B. J. Berne and R. Pecora, *Dynamic Light Scattering* (Wiley, New York, 1976).
9. E. O. Schulz-Dubois, in *Photon Correlation Techniques in Fluid Mechanics*, E. O. Schultz-DuBois ed., 6 (Springer-Verlag, Berlin, 1983).
10. E. J. Hinch, *J. Fluid Mech.*, **72**, 499 (1975).
11. For a recent review on photon localization theory and experiment see S. John, *Physics Today*, **44**, 32 (1991) and references therein.
12. For a recent review on speckle correlation functions see S. Feng and P. A. Lee, *Science*, **251**, 633 (1991) and references therein.
13. Our derivation basically follows the discussion in D. J. Pine, D. A. Weitz, J. X. Zhu, and E. Herbolzheimer, *J. Phys. France*, **51**, 2101 (1990).
14. This calculation involves the so called $C^{(1)}$, $C^{(2)}$, and $C^{(3)}$ intensity-intensity correlation functions. Detailed discussion and measurement of these functions can be found in S. Feng, C. Kane, P. A. Lee and A. D. Stone, *Phys. Rev. Lett.*, **61**, 834 (1988); N. Garcia and A. Z. Genack, *Phys. Rev. Lett.*, **63**, 1678 (1989); M. P. van Albada, J. F. de Boer and A. Lagendijk, *Phys. Rev. Lett.*, **64**, 2787 (1990).
15. D. J. Pine and A. G. Yodh unpublished.
16. H. S. Carslaw, and J. C. Jaeger, *Conduction of Heat in Solids*, 2nd Edition (Clarendon Press, Oxford, 1959).
17. A. G. Yodh, P. D. Kaplan, and D. J. Pine, *Phys. Rev.*, **B42**, 4744 (1990).
18. See for example J. Shah, *IEEE J. Quant. Electron.*, **24**, 276 (1988); R. Vreeker, M. P. Van Albada, R. Sprik, and A. Lagendijk, *Phys. Lett.*, **A132**, 51 (1988); K. M. Yoo, Y. Takiguchi, and R. R. Alfano, *Appl. Opt.*, **28**, 2343 (1989).
19. D. A. Weitz, D. J. Pine, P. N. Pusey, and R. J. A. Tough, *Phys. Rev. Lett.*, **63**, 1747 (1989).
20. A. G. Yodh, N. Georgiades, and D. J. Pine, *Opt. Commun.*, **83**, 56 (1991).
21. M. Born and E. Wolf, *Principles of Optics* (Pergamon Press, New York, 1980).
22. R. Zwanzig and M. Bixon, *Phys. Rev.*, **A2**, 2005 (1970); R. Zwanzig and M. Bixon, *J. Fluid Mech.*, **69**, 21 (1975); B. J. Alder and T. E. Wainwright, *Phys. Rev. Lett.*, **18**, 988 (1967); B. J. Alder and T. E. Wainwright, *Phys. Rev.*, **A1**, 18 (1970).
23. X. Qui, X. L. Wu, J. Z. Xue, D. J. Pine, D. A. Weitz and P. M. Chaikin, *Phys. Rev. Lett.*, **65**, 516 (1990).
24. S. Fraden and G. Maret, *Phys. Rev. Lett.*, **65**, 520 (1990).
25. F. C. MacKintosh and S. John, *Phys. Rev.*, **B 40**, 2383 (1989).
26. B. J. Ackerson, *J. Chem. Phys.*, **64**, 242 (1976); B. J. Ackerson, *J. Chem. Phys.*, **89**, 684 (1978).
27. T. Biben and J. P. Hansen, *Phys. Rev. Lett.*, **66**, 2215 (1991); J. L. Barat, M. Baus and J. P. Hansen, *J. Phys. C: Solid State Phys.*, **20**, 1413 (1987).
28. P. Bartlett, R. H. Ottewill and P. N. Pusey, *J. Chem. Phys.*, **92**, 1299 (1990); P. N. Pusey, H. M. Fijnaut and A. Vrij, *J. Chem. Phys.*, **77**, 4220 (1982).
29. S. W. Rick and A. D. J. Haymet, *J. Chem. Phys.*, **90**, 1188 (1989).
30. M. J. Murray and J. V. Sanders, *Phil. Mag.*, **A42**, 721 (1980).
31. Relevant details concerning the Percus-Yevick approximation and its extension to binary hard sphere systems can be found in J. L. Lebowitz, *Phys. Rev.*, **133**, 895 (1964); N. W. Ashcroft and D. C. Langreth, *Phys. Rev.*, **156**, 685 (1967); N. W. Ashcroft and D. C. Langreth, *Phys. Rev.*, **159**, 500 (1967).
32. G. K. Batchelor, *J. Fluid Mech.*, **74**, 1 (1976).
33. P. N. Pusey and R. J. A. Tough, *J. Phys. A: Math Gen.*, **15**, 1291 (1982).
34. D. J. Durian, D. A. Weitz and D. J. Pine, *Science*, **252**, 686 (1991).